POLITECNICO
MILANO 1863

SCUOLA DI INGEGNERIA INDUSTRIALE
E DELL'INFORMAZIONE

Executive Summary of the Thesis

Preliminary studies on heavy metals accumulation at nano-scale in the shell of *Patella caerulea*

Laurea Magistrale in Engineering Physics - Ingegneria Fisica

Author: Federico Castelli

Advisor: Prof. Giacomo Claudio Ghiringhelli

Co-advisor: Madeleine Han

Academic year: 2022-2023

1. Introduction

Mollusks, and in particular the shell structure, are highly sensitive to environmental conditions, making them a valid subject for biomonitoring studies. Different alterations are observed in the shell structure after exposure to a polluted environment, both in shape and composition of the shell. In particular, chemical alterations of the main constituents of the shell (Ca, C, P, S), together with trace metals accumulation, are usually employed as valid parameters for assessing the quality of sea water. The accumulation of trace metals in the shell is considered as an active mechanism adopted by the mollusk to excrete toxic elements from the soft body. The vast majority of the studies measure the overall chemical composition of the shell for biomonitoring purposes. Few studies reported a spatially resolved chemical analysis at μ-scale, but considering only major constituents of the shell. Furher insights would be provided by analyzing the chemical composition at nano-scale, possibly clarifying the way trace metals incorporate in the shell structure and in which regions they accumulate. In the present study both nano X-Ray Fluorescence (XRF) and nano-tomography techniques were employed in synergy, to assess the composition of different shell samples of the species *Patella caerulea*. The shells were analyzed all along their width, from the outermost layer to the inner most one. XRF technique would provide a direct measure of the distribution of different elements with high spatial resolution. Nano-tomography would provide complementary results, by possibly revealing inhomogeneities in the shell structure associated to trace metals.

2. XRF technique

XRF technique is a photon in-photon out techniques which allows to determine and quantify the chemical composition of the sample, providing a 2D chemical map. The principle behind this technique relies on the unique set of electronic energy levels that characterize each atom. An X-ray beam is focused on the samples exciting electrons from different atoms composing the specimen. Subsequently to excitation, the atoms relax by emitting fluorescence radiation, characterized by an energy equal to the difference between the energies of the two electronic states involved in the relaxation process. Detecting the fluorescence radiation emitted allows

to identify the chemical composition of the sample. In the present study, synchrotron radiation XRF allowed to achieved sub-ppm detection limits for different elements, providing a significant quantification, together with a high spatial resolution of 200 nm. The X-ray beam energy was set to 29.6 keV so that K emission lines of heavy-metals up to Sn ($K_{\alpha 1} = 25.27keV$) could be excited.

3. Multi-distance tomography technique

Tomography technique allows to retrieve the 3D mass density distribution ρ of a sample by exploiting X-rays. The incoming X-ray field Ψ_{IN} is propagated through the sample, resulting in the field Ψ_{OUT} at the exiting surface of the object, which encodes information about the complex refractive index of the sample:

$$n(x, y, z) = 1 - \delta(x, y, z) + i\beta(x, y, z) \qquad (1)$$

where the real part is associated to the mass density ρ of the sample. A further propagation of the wave field Ψ_{OUT} along a distance Δ, where a position sensitive detector is placed, allows the intensity contrast to develop, so that the measured field intensity $I_\Delta = |\Psi_\Delta|^2$ reveals a phase-contrast pattern. Employing the Paganin formula [1] to solve the inverse problem of phase retrieval, is possible to obtain the 2D phase map of the wave field Ψ_{OUT}. Determining the 2D phase map over different angular position of the sample, allows to reconstruct the 3D complex refractive index employing a suitable algorithm. In particular, an iterative algorithm based on alternating projections was employed for the reconstruction in the present study. Considering the already significant spatial resolution of 50 nm achieved relying on synchrotron radiation source, a multi-distance approach was exploited to further improve the spatial resolution and obtain a better phase contrast across all spatial frequencies, reducing the effects of the noise.

4. Samples analyzed

Two samples of shell of the species *Patella caerulea* were effectively considered in the analysis. In particular, the samples were collected[1] from different geographical areas among which a gradient of pollution was reported. Sample G0 was collected from the harbor area of the city of Gabes (Tunisia), known to be a highly polluted site. Sample Z1 was collected from the harbor area of Zarat (Tunisia), where a lower seawater pollution was reported.

5. Results and discussion

Experiments were conducted at the nano-probe beamline ID16B at the European Synchrotron Radiation Facility in Grenoble, France.

5.1. Assessing the levels of pollution in the shells

A first analysis of the XRF maps was conducted to quantify the overall composition of the shells, neglecting the spatial resolution. In this way, the levels of pollution of the samples were determined to provide a basis for the subsequent analysis. An intra-study comparison showed sample G0 to present a slightly higher concentration of different trace metals (Fe, Cr, Co, Ni, Mn) with respect to sample Z1, in accordance with the higher pollution of Gabes area. Contrarily, sample Z1 reported slightly higher concentrations of Sn and Zr. The remaining trace elements identified in the shells (Cu, Cd, Zn, W, Ag, Br, As and Ge) were present in equal concentration in the samples, suggesting a similar contamination. An inter-study comparison with results reported in literature suggested a strong contamination for both samples concerning Fe, Cr, Co, Mn, Sn, Cu and Zn.

5.2. Accumulation along growth lines

A Ca-Sr substitution was observed in concomitance of regions identified as growth lines, present at the interface between consecutive shell layers. A Pearson correlation analysis corroborated the Ca-Sr substitution providing a significant anti correlation ($r_{G0} = -0.62$, $r_{Z1} = -0.64$). Additionally, the correlation analysis suggested a substitution of W for sample G0 and Br for both samples, with Ca. This substitution was again localized in concomitance of the growth lines as shown inFigure 1. Differently, the 3D rendering obtained from nano-

[1] Samples were provided by Youssef Lahbib, Université de Carthage, Faculté des Sciences de Bizerte

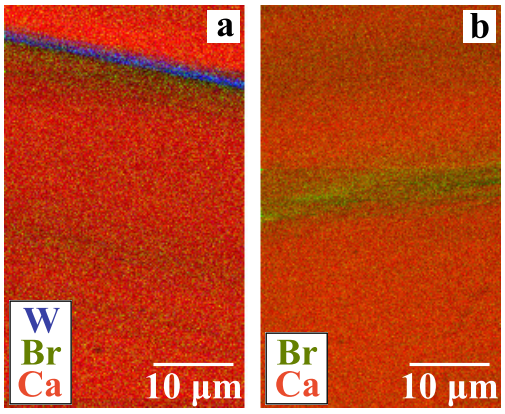

Figure 1: XRF maps showing presence of Br and W accumulated along growth lines. (a) represent one XRF map from sample G0. (b) represents one XRF map from sample Z1.

tomography showed a smaller density in concomitance of the growth lines, either suggesting presence of porosities within these regions or hinting a strong accumulation of light elements, not detected by XRF technique.

5.3. Trace metals accumulation

The spatial resolution achieved with nano-XRF allowed to identify different inhomogeneities in the elemental maps of Cu, Fe, Sn, Zn and Zn, even though their presence was not suggested by the correlation analysis. In particular, different localized regions were observed, ranging from 200 nm up to $\approx$ 20 μm, where a higher concentration of these elements was present, as shown in Figure 2.

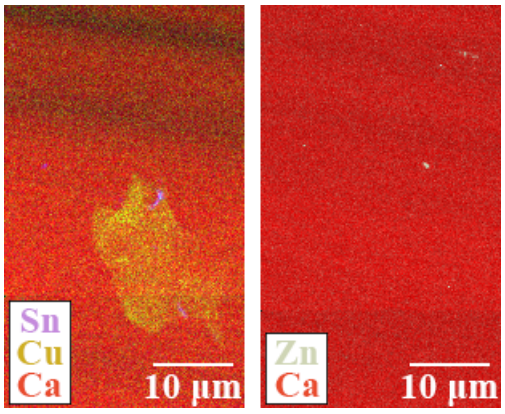

Figure 2: Example of two XRF maps obtained from sample G0 showing metallic agglomerates.

These metallic agglomerates were manually measured employing ImageJ software and catalogued. The results obtained showed more numerous metallic agglomerates for sample G0, in agreement with the expected higher contamination of this sample. In particular, Cu, Fe Ag agglomerates were identified only in sample G0, while Sn and Zn were identified in both samples. Unfortunately, the small collection of these agglomerates didn't allow to conduct any statistics about their localization within the samples. Further analysis on other samples would provide the possibility compute a significant statistics.

5.4. Inhomogeneous distribution of pores in the shell structure

Nano-tomography was expected to possibly reveal local changes in density related to the presnce of trace metals, corroborating the results from XRF analysis. Instead, the bulk region of the shell was characterized by spherical nano and micro-scale low-density regions, considered as pores. The distribution of the pores and their sizes were inhomogeneous inside the structure, identifying regions with an enhanced concentration. A further segmentation and calculation of the pores sizes within different volumes of the sample provided a clear proof of this qualitative observation, as shown in Figure 3.

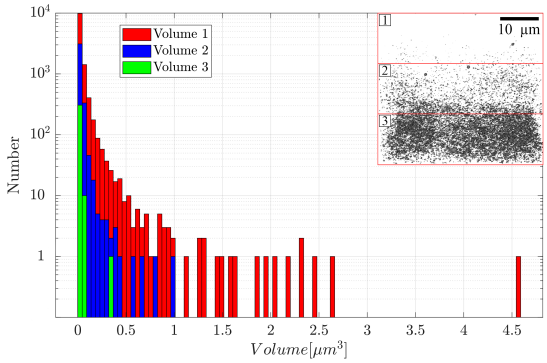

Figure 3: The histogram reports the statistics of the pores volume within three different subvolumes of the shell. The inset shows a lateral view of the 3D rendering of the pores in the three sub-volumes.

The enhanced presence of pores in different regions was hypothesized to be caused by an erroneous mineralization associated to a failure of the filling mechanism of Ca^{2+} proposed by Chang-Yu et al. [2]. Environmental stressors were possibly associated to the erroneous mineralization. If pollution was the cause, a higher concentration of trace metals was expected in

concomitance of this pores-enriched regions. A first qualitative comparison didn't shown any evident correlation. Further analysis should be performed to rigorously assess a possible correlation.

5.5. Enhanced metal accumulation in outer shell layer micro cavities

Both XRF maps and nano-tomography 3D rendering showed the existence of micro-cavities in the outer layer of the shell, already observed in other studies and associated to fouling activity of micro-organisms. The sensitivity achievable with synchrotron XRF allowed to identify a variety of trace elements, such as Fe, Co, Ni, Cu, Zn, W, Br and Ge, localized inside the cavities, as shown in Figure 4.

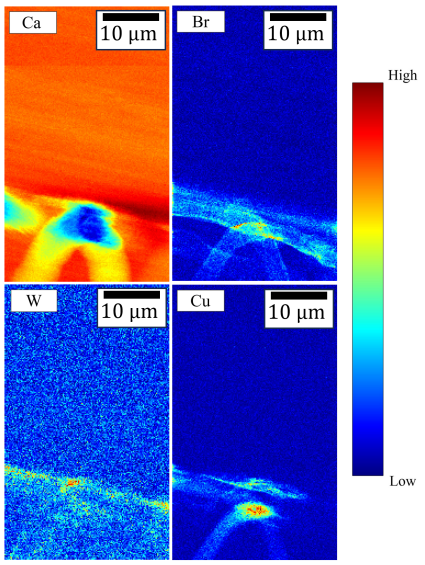

Figure 4: Ca distribution in the outer layer suggested the presence of holes in the shell structure. Example of different trace elements observed inside the micro-cavities.

Nano-tomography images only showed less dense regions, suggesting that the cavities were effectively characterized by an empty volume inside. No hints of trace elements accumulation were suggested by nano-tomography, possibly associated to the different sensitivity compared to XRF. The direct exposure of the outer layer to the surrounding environment, together with the morphology of the cavities, justified the enhanced uptake of metals, possibly involving an initial surface adsorption and a consequent diffusion into the cavities.

5.6. Conclusions and perspectives

Nano-XRF technique identified an accumulation of Sr, W and Br in concomitance of different growth lines in the shell structure. Sr is known to easily substitute Ca due to their atomic similarity, while W and Br were possibly accumulated in these regions due to a strong environmental pollution.
The nano-scale spatial resolution achieved with XRF provided a first direct proof of trace metals accumulation in forms of μm and sub-μm agglomerates inside the shell structure. The larger abundance in one sample was congruent with the higher levels of pollution identified by quantification analysis. The small overall number of agglomerates identified didn't allow to conduct a significant statistics concerning their localization inside the shell, requiring further analysis on more samples and possibly in different regions of the shell (tip and middle flank region).
Nano-tomography analysis revealed a inhomogeneous distribution of spherical nano-scale and micro-scale pores inside the shell structure, not reported in literature before. Their inhomogeneous distribution along the shell width suggested that at specific times during the growth of the calcified layer, the mollusk suffered from environmental stress, possibly associated to heavy-metals pollution. A first qualitative comparison between the distribution of trace metals and the pores didn't shown any evident correlation. Further analysis should be performed to rigorously assess a possible correlation.
The outer layer of the shell showed an enhanced accumulation for different trace elements. The presence of micro-cavities within this layer, ascribed to fouling activity by micro-organisms, probably promoted the significant accumulation observed, making this shell region suitable for biomonitoring studies.

6. Acknowledgements

I would like to thank our collaborator Youseff Lahbib who provided us the samples and made possible the present study. Also a special thanks to all the colleagues from ID16B beamline who supported me, providing advice during the analysis of the data. A profound thanks to my supervisor Madeleine who helped throughout all my traineeship at ID16B.

References

[1] David M. Paganin and Daniele Pelliccia. Chapter two - x-ray phase-contrast imaging: a broad overview of some fundamentals. In *Advances in Imaging and Electron Physics*, Advances in Imaging and Electron Physics. Elsevier, 2021.

[2] Chang-Yu Sun, Cayla Stifler, Rajesh Chopdekar, Connor Schmidt, Ganesh Parida, Vanessa Schoeppler, Benjamin Fordyce, Jack Brau, Tali Mass, Sylvie Tambutté, and Pupa Gilbert. From particle attachment to space-filling coral skeletons. *Proceedings of the National Academy of Sciences*, 117, 11 2020.